

Orientation and Relaxation Study of Miscible Polystyrene/Poly(vinyl methyl ether) Blends

Christian Pellerin, Robert E. Prud'homme, and Michel Pézolet*

Centre de recherche en sciences et ingénierie des macromolécules, Département de chimie, Université Laval, Québec, Canada G1K 7P4

Received February 16, 2000; Revised Manuscript Received July 13, 2000

ABSTRACT: The macroscopic deformation and relaxation of orientation of miscible polystyrene/poly(vinyl methyl ether) (PS/PVME) blends containing between 50 and 100% PS have been studied using polarization modulation infrared linear dichroism (PM-IRLD). PS/PVME films were stretched at $T_g + 15$ to a draw ratio of 2, at constant draw rates of 10 and 100 cm/min. During the deformation, the addition of the lower molecular weight PVME to the blends leads to an important increase of the orientation function of PS. During the relaxation period, a fast decay of the PS orientation function occurs at short times, followed by a slow chain relaxation at longer times. The relaxation rate is faster in pure PS than in the blends, the increase of the PVME content leading to a hindered relaxation. The orientation function of PVME is small in all cases, but we have been able, for the first time, to measure directly its relaxation, which follows closely the trend observed for PS. However, no relaxation coupling can be clearly observed between the two polymers, the relaxation rate of PVME being always faster than that of PS. These results demonstrate the efficiency of PM-IRLD to determine quantitatively the time dependence of the orientation function of several chemical groups in multicomponent systems during the orientation and relaxation processes.

Introduction

Molecular orientation induced during the processing of polymers has a significant impact on their physical properties. It is thus important to understand the deformation and relaxation mechanisms at a molecular level in order to obtain high-performance polymers. For homopolymers, the deformation process has been relatively well characterized.^{1–3} However, in the important field of polymer blends, our understanding is still embryonic due to the complex interactions between the components.

Monnerie et al. have observed that, in miscible polystyrene/poly(2,6-dimethyl-1,4-phenylene oxide) (PS/PPO) blends, the addition of a second component induces a higher orientation of the initial polymer.^{4,5} In blends of PS with poly(vinyl methyl ether) (PS/PVME), an increase of PS orientation with PVME content has also been reported by Monnerie et al. and by Abtal and Prud'homme, but the orientation of PVME could not be determined directly.^{6,7} These results were interpreted by an increase of the friction coefficient between the two species involved due to the specific interactions that are at the origin of their miscibility. Zhao et al. have also studied PS/PPO blends, but they suggested that the increase in orientation was the consequence of a higher entanglement density in the blends.⁸ Indeed, a relaxation coupling between the two blend components has been observed in the PS/PPO system and in other blends by indirect⁹ or direct¹⁰ methods.

The relaxation of orientation that occurs during and after the deformation of polymer blends is not well understood due to the lack of experimental techniques able to follow its rapid kinetics. Birefringence can be used for that purpose, but it cannot discriminate

between the different blend components. Infrared linear dichroism (IRLD) has been widely used to study polymer deformation because it can differentiate between the components of polymer blends or between the different phases of semicrystalline polymers, but it has a very limited time resolution. To improve its sensitivity and time response, IRLD has been recently coupled with the polarization modulation (PM) technique.^{11,12} The use of PM-IRLD enables the quantitative determination of the orientation and relaxation kinetics of different blend components because the dichroic difference spectra are recorded directly in real time, thus minimizing instrumental and sample fluctuations. PM-IRLD has been successfully used to study the light-induced orientation of azopolymers^{13,14} and, more recently, the orientation relaxation of a series of monomolecular PS¹⁵ and of PS/PPO blends.¹⁰

In this work, we have used PM-IRLD to study the macroscopic deformation and the relaxation of orientation of miscible PS/PVME blends containing between 50 and 100% PS stretched uniaxially above their glass transition temperature (T_g). For the first time, we have been able to follow directly the relaxation of orientation of both PS and PVME, after a deformation at $T_g + 15$ at draw rates of 10 and 100 cm/min. This blend is completely amorphous, i.e., no complication should arise from a crystalline phase, and it can be prepared in the miscible state by using an appropriate solvent.¹⁶ Its miscibility is due to the presence of specific interactions between the phenyl groups of PS and methoxy side chains of PVME.^{17,18} This blend can also be phase-separated with a controlled morphology by heating above its lower critical solution temperature (LCST).^{19,20} Therefore, it constitutes an interesting model for polymer blends.

Experimental Section

Monodisperse atactic polystyrene (Pressure Chemical) with $M_w = 942$ kg/mol and poly(vinyl methyl ether) (Polymer

* Corresponding author. Tel (418) 656-2481; Fax (418) 656-7916; E-mail Michel.Pezolet@chm.ulaval.ca.

Scientific Products) with $M_w = 59$ kg/mol were used. The polydispersity index of PVME was reduced to 1.3 by precipitation fractionation, as determined by size exclusion chromatography (Waters model 590) in tetrahydrofuran. Self-supported films containing from 50 to 100% w/w PS were cast on a glass plate from 3% benzene solutions. The thickness of the samples was adjusted between 30 and 60 μm to ensure an absorbance below unity for the infrared bands investigated. Films were air-dried at room temperature for 2 days and then gradually heated under vacuum up to $T_g + 30$ for at least 48 h to remove the last traces of solvent and residual stresses. T_g 's were determined as the midpoint of the heat capacity jump by differential scanning calorimetry (Perkin-Elmer DSC-7) at a scanning rate of 10 K/min. A linear relation between T_g and PS content was observed: the T_g 's were 105, 87, 67, 43, 20, and 2 $^\circ\text{C}$ for samples containing 100, 90, 80, 70, 60, and 50% PS, respectively. The samples were cut into strips having 20 mm in length and 6 mm in width and marked with ink lines to verify the real draw ratio. A pyrotape (Aremco Products No. 546) was used to avoid the slippage of the films during the elongation.

PS/PVME films were stretched to a fixed draw ratio of 2 at $T_g + 15$ at a constant draw rate of 10 or 100 cm/min, using mechanical stretchers fitted with ZnSe windows to allow the in situ recording of the PM-IRLD spectra during the orientation and relaxation periods. The first stretcher used, as previously described, allows deformation of films at draw rates below 10 cm/min.²¹ The second stretcher, recently developed in our laboratory, is driven by a stepper motor and can be used to deform samples at draw rates ranging from 10 up to 1200 cm/min at temperatures between 0 and 170 $^\circ\text{C}$. The temperature was adjusted using an Omega temperature controller (CN 7600) and heating cartridges. For experiments below room temperature, liquid nitrogen-cooled nitrogen was circulated through the walls of the stretcher. In every cases, the temperature control was better than 0.5 $^\circ\text{C}$. Dichroic difference spectra with a resolution of 8 cm^{-1} were obtained using a Bomem Michelson MB-100 spectrophotometer using the optical setup and the two-channel electronic processing described previously.¹⁴ A ZnSe photoelastic modulator (Hinds PEM-90 type II/ZS50), operating at 50 kHz, a lock-in amplifier (EG&G 7260 DSP) with a 40 μs time constant, and two dual-channel electronic filters (Stanford Research Systems SR650) were used to generate the double modulation and to isolate the experimental signals. MCT (Belov) and InSb (EG&G Judson) detectors cooled with liquid nitrogen were used for the low- and high-frequency experiments, respectively. All the experiments were conducted in three consecutive acquisition steps: the first series of 180 spectra of 4 scans was followed by 90 spectra of 30 scans and by a final series of 80 spectra of 75 scans.

The order parameter or orientation function $\langle P_2 \rangle$ was calculated from the intensity of the dichroic difference ΔA as²²

$$\langle P_2 \rangle = \frac{2}{3\langle \cos^2 \alpha \rangle - 1} \frac{\Delta A}{3A_0} \sqrt{\lambda} \quad (1)$$

where λ is the draw ratio, A_0 is the absorbance of the unstretched isotropic sample, and α is the average angle between the transition moment of the vibration considered and the main chain axis. The relaxation curves obtained at a 100 cm/min draw rate were used to determine experimental relaxation times by minimizing the least-squares difference between the experimental and calculated curves, using the built-in solver of Microsoft Excel.

Results

In a first series of experiments, PS/PVME films were deformed at $T_g + 15$ at a stretching rate of 10 cm/min. Figure 1 shows the infrared spectrum of the initial undeformed sample of a 90/10 blend in the low-frequency region and three dichroic difference spectra recorded immediately at the end of the deformation (0

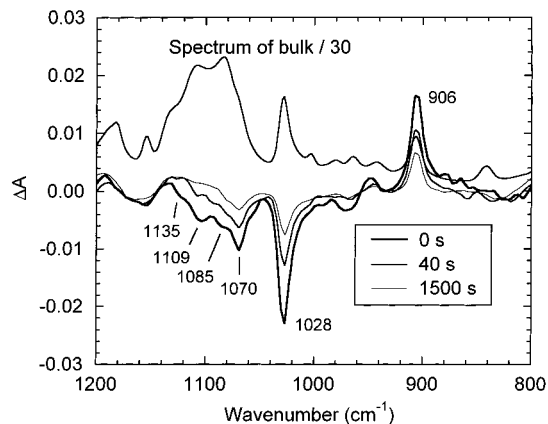


Figure 1. Infrared spectrum of an undeformed 90/10 PS/PVME blend in the low-frequency region and dichroic difference spectra recorded at the end of the deformation (0 s) and after 40 and 1500 s of relaxation ($T_g + 15$, 10 cm/min).

s) and after 40 and 1500 s of relaxation. The signal-to-noise ratio in these spectra is excellent even if the number of scans per spectrum was limited, and the maximum ΔA is less than -0.03 . The acquisition time necessary to obtain the spectra at 0 and 40 s was 1.6 s only. This demonstrates unambiguously the high sensitivity of the PM-IRLD technique to follow orientation dynamics. Clearly, the dichroic difference of all bands of Figure 1 decreases with time as the macromolecular chains relax to their isotropic state.

The two PS bands observed at 906 and 1028 cm^{-1} are well resolved and are assigned to the ν_{17b} out-of-plane and ν_{18a} in-plane vibrations of the phenyl ring, respectively. These two vibrations are considered to be insensitive to the conformation of the polymer, and the angle α between their transition moment and the chain axis is 35 $^\circ$ and 90 $^\circ$, respectively.² Since the chains orient along the stretching direction, the 1028 cm^{-1} band appears as a negative peak in the dichroic difference spectra because its transition moment is perpendicular to the chain axis. In the region between 1050 and 1150 cm^{-1} , the 1070 cm^{-1} band of PS, due to the ν'_{18b} vibration, strongly overlaps with three intense bands of PVME at 1085, 1109, and 1135 cm^{-1} , all associated with the C–O–C stretching of the methoxy side chain. In the spectrum of the undeformed sample, the 1070 cm^{-1} PS band appears as a shoulder even though the blend contains only 10% PVME. However, the trend is reversed in the dichroic difference spectra, in which it becomes prominent. This indicates that, during the deformation of this blend, the PS chains acquire a significant orientation while the chains of the soft PVME remain poorly oriented.

The chain order parameter $\langle P_2 \rangle$ of PS can be determined quantitatively from eq 1 for both the 906 and 1028 cm^{-1} bands, but only the second one has been used in this work. Figure 2 shows the variation of $\langle P_2 \rangle$ with the draw ratio during the deformation process of PS/PVME blends containing between 50 and 100% PS. A linear increase of $\langle P_2 \rangle$ with the draw ratio is found for all samples. It can be observed that pure amorphous PS exhibits a low level of orientation as compared to other homopolymers at the same temperature relative to T_g .^{23,24} At the end of the deformation process, the order parameter of PS is 0.03 only, while a perfect orientation would give a $\langle P_2 \rangle$ value of 1. It is important to note the low scatter of the data in these curves as compared to those obtained by IRLD. This improvement

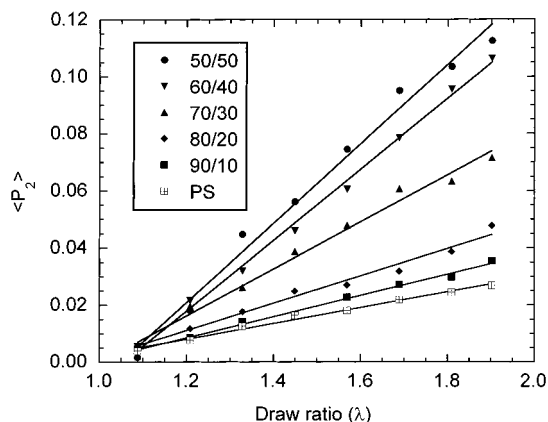


Figure 2. Orientation function $\langle P_2 \rangle$ of PS (1028 cm^{-1} band) in blends containing 50–100% PS as a function of the draw ratio λ , at $T_g + 15$ and at 10 cm/min .

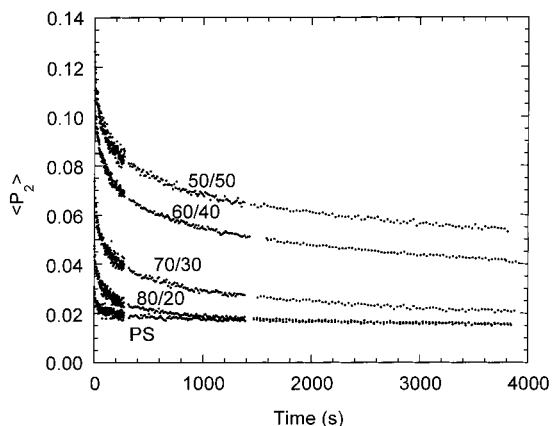


Figure 3. Relaxation curves of PS (1028 cm^{-1} band) in blends containing 50–100% PS as a function of time after a deformation at $T_g + 15$ and at 10 cm/min .

is possible because the dichroic difference spectra are measured directly in PM-IRLD experiments without the artifacts introduced by polymer relaxation during the acquisition (or during the quenching) or instrumental instabilities. Furthermore, it is possible to measure very low levels of orientation with PM-IRLD, like those encountered in amorphous polymers at small draw ratios above T_g .

The addition of PVME to the blends leads to an important increase of the order parameter of PS. In the 50/50 blend, the orientation at the end of the deformation is in fact more than 4 times higher than in the pure polymer. It can be noted in Figure 2 that the orientation increase is small for the blends containing 10 or 20% PVME and it becomes much larger at 70/30 and 60/40 compositions, while the additional increase in the 50/50 blend is modest. These results are in good agreement with the measurements of Abtal and Prud'homme, in which a maximum orientation was observed in the 50/50 blend.⁷

Figure 3 shows the relaxation curves of PS in the same PS/PVME blends. The relaxation curve of the 90/10 blend is omitted for clarity, but it fits perfectly between the 80/20 blend and pure PS. As expected, a fast decay is observed at short times, while a slow chain reorientation occurs at longer times. It can be seen that the relaxation rate is faster in pure PS than in the different blends, the increase of the PVME content leading to a hindered relaxation. The final orientation, at about 4000 s, is practically the same for the three

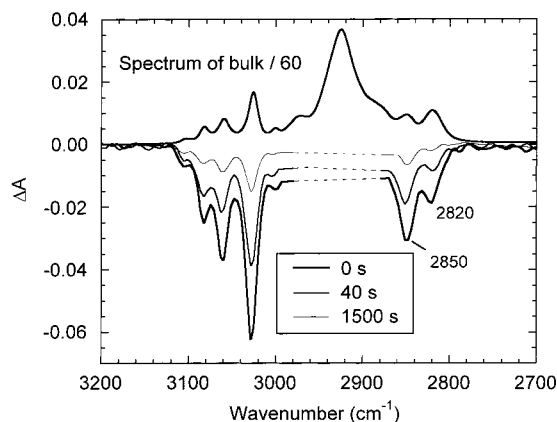


Figure 4. Infrared spectrum of an undeformed 70/30 PS/PVME blend in the high-frequency region and dichroic difference spectra recorded at the end of the deformation (0 s) and after 40 and 1500 s of relaxation ($T_g + 15$, 100 cm/min). The dashed region was erased in the dichroic spectra because the bands were saturated.

PS-rich samples. However, it increases significantly for blends containing 70, 60, and 50% PS, as observed in Figure 2 in the orientation data. A variation of the friction coefficient, as proposed in the literature,^{6,7} could explain the results of Figures 2 and 3: an increase of the friction coefficient between the dissimilar polymer chains should lead to a limited mobility of the two components and, thus, to a hindered relaxation, as is observed here for PS. However, this evidence does not rule out other possible explanations, as will be discussed later.

Even if the dichroic spectra of Figure 1 give a qualitative indication that the level of orientation of PVME is very low in these blends, it was not possible to determine its order parameter from measurements in the low-frequency region. The PVME bands strongly overlap with the more oriented PS absorption band, and their strong intensity in the spectrum before stretching requires the use of very thin films to keep the absorbance below unity, making these films difficult if not impossible to stretch. Actually, the low PVME orientation can result from a higher relaxation rate than PS or to a smaller intrinsic orientation. It has been shown, for instance, that in the PS/PPO system the low- T_g component possesses a smaller intrinsic orientation when exposed to a given external stress, but nevertheless, the two polymers relax in a cooperative fashion with the same characteristic times.⁸

To provide an answer to this question, a series of experiments were conducted using a photovoltaic InSb detector, that is extremely sensitive in the high-frequency region of the mid-infrared, to measure the orientation relaxation of PS/PVME blends in the C–H stretching region. In these experiments, a rapid stretching rate of 100 cm/min has been chosen to minimize the relaxation of orientation of PVME during the deformation and to facilitate the measurement of its dichroic difference. Figure 4 shows, as an example, the infrared spectrum of an undeformed 70/30 blend and three dichroic difference spectra recorded immediately at the end of the deformation (0 s) and after 40 and 1500 s of relaxation. The 2920 cm^{-1} band, due to the superposition of strong backbone absorptions of PS and PVME, was eliminated (dotted lines) in the dichroic spectra because it was saturated. Once again, the signal-to-noise ratio is excellent in these spectra. Two bands were

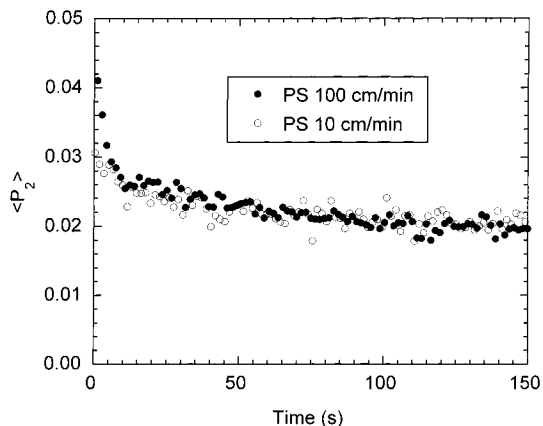


Figure 5. Relaxation curves of two pure PS samples as a function of time after a deformation at 10 cm/min (1028 cm^{-1} band) and 100 cm/min (2850 cm^{-1} band), at $T_g + 15$.

selected in this region in order to follow the relaxation dynamics of both blend components. The 2850 cm^{-1} PS band is assigned to the CH_2 symmetric stretching, while the 2820 cm^{-1} PVME band is related to the methoxy side chain CH_3 symmetric stretching. There is a certain overlap between these bands in the spectrum of the initial sample, but it can be shown that the contribution of the PS band in the 2820 cm^{-1} region is negligible in the dichroic difference spectra. Both bands appear as negative peaks, indicating that their transition moment is perpendicular to the main chain. An α angle of 90° has been assumed for these two bands.²⁵ As observed in Figure 1 for the 90/10 blend, the dichroic difference of the PVME band is always smaller than that of PS, while its intensity is higher in the spectrum undeformed sample, suggesting a lower level of orientation.

Since the total stretching time is about 1.3 s only at a draw rate of 100 cm/min, it was not possible to determine the $\langle P_2 \rangle$ values during the deformation process. However, such a short time provides a better accuracy in the initial part of the relaxation curves. This behavior is clearly illustrated in Figure 5, where are compared the relaxation curves of two pure PS samples stretched at the same temperature and draw ratio, but at either 10 or 100 cm/min. The initial orientation of the PS sample deformed at a higher rate is significantly larger than that of the other sample and is followed by a very fast relaxation during the first 10 s. After a few tens of seconds, the two curves become identical within the experimental error. This comparison demonstrates that the two mechanical stretchers used in this study give consistent results.

The relaxation curves of PS in the different blends have also been measured using the 2850 cm^{-1} band, and the results obtained (not shown) are in good agreement with the curves of Figure 3 obtained with the 1028 cm^{-1} band. Figure 6 shows the relaxation curves of PS (with the 2850 cm^{-1} band) and PVME (2820 cm^{-1} band) in PS/PVME blends containing 60 and 70% PS, at $T_g + 15$. To our knowledge, this is the first direct determination of the relaxation curve of PVME in PS/PVME blends. The orientation level of PS appears to be significantly higher than that of PVME in the two blends, but care must be taken when comparing the absolute $\langle P_2 \rangle$ values because the α angle of PVME is not known with accuracy.⁶ However, it is obvious from Figure 6 that the addition of PVME to PS in the blends leads to an important increase of the orientation not

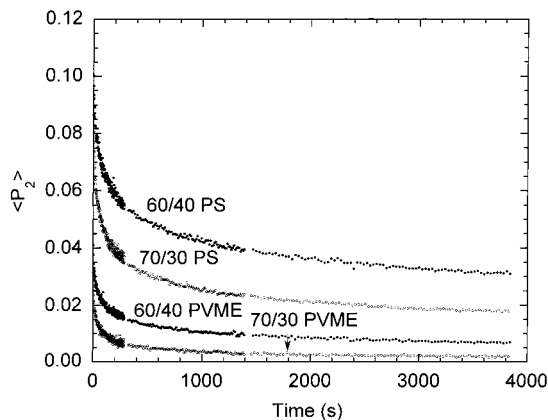


Figure 6. Relaxation curves of PS (2850 cm^{-1} band) and PVME (2820 cm^{-1} band) in the 60/40 and 70/30 blends as a function of time, after a deformation at $T_g + 15$ and at 100 cm/min.

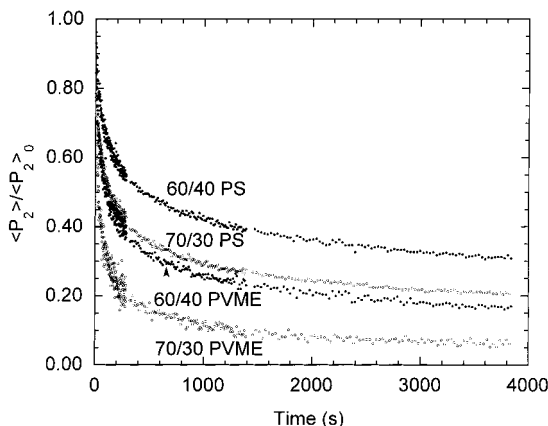


Figure 7. Normalized relaxation curves of PS (2850 cm^{-1} band) and PVME (2820 cm^{-1} band) in 60/40 and 70/30 blends as a function of time, after a deformation at $T_g + 15$ and at 100 cm/min.

only of PS, as already seen in Figures 2 and 3, but also of PVME since, when going from the 70/30 to the 60/40 blend, the order parameter of PVME becomes much higher. A lower PVME orientation is detected for the blends containing 20% PVME (not shown), while no significant dichroism was measured in the 90/10 blend. Since the order parameter of PVME decreases rapidly with time to reach a very small value, such results cannot be obtained by conventional infrared linear dichroism. Finally, it was not possible to perform experiments with 50/50 blends because the strong absorbance of PVME required samples too thin to be stretched.

Figure 7 shows the relaxation curves of PS and PVME in the 60/40 and 70/30 blends normalized relative to the first data point at time zero. Since the PS and PVME orientation functions were measured from the same sample, the normalization process allows the comparison of the relative relaxation rate of the different polymers without the uncertainties related to the exact draw ratio. This figure shows that the relaxation of both PS and PVME is hindered in the 60/40 blend as compared to the 70/30 blend.

Discussion

The molecular relaxation of a chain in a melt can be considered as the sum of two contributions: the intrinsic relaxation of the chain and a relaxation coupling with the surrounding matrix. Since, in this work, the relax-

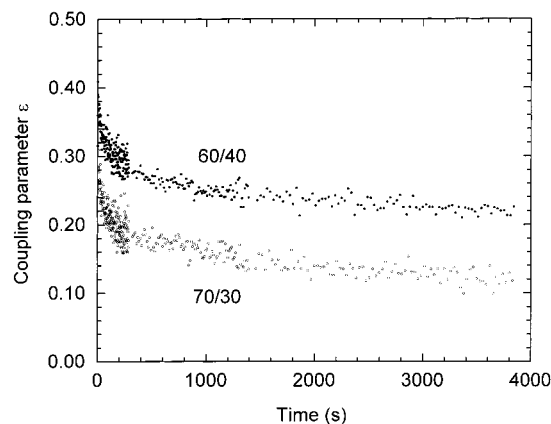


Figure 8. Coupling parameter ϵ (as determined by eq 2) of 60/40 and 70/30 blends as a function of time, after a deformation at $T_g + 15$ and at 100 cm/min.

ation curves of PS and PVME have been determined independently, it is possible in that framework to define a coupling parameter ϵ as

$$\frac{\langle P_2 \rangle_{\text{PVME},t}}{\langle P_2 \rangle_{\text{PS},t}} = \epsilon \quad (2)$$

where $\langle P_2 \rangle_{i,t}$ is the order parameter of polymer i at time t . A constant ϵ value with time would be indicative of a strong relaxation coupling between the two polymers: even if their orientation function is different, they may relax at the same rate. As shown in Figure 8, ϵ values calculated from Figure 7 and eq 2 vary as a function of time from about 0.41 to 0.22 in the 60/40 blend and from 0.36 to 0.12 in the 70/30 blend. This decrease of ϵ with time, particularly at short times, means that the relaxation is not cooperative, as qualitatively estimated from Figure 7. Even at 4000 s, a plateau is not reached, indicating that PVME still relaxes faster than PS even if the blends are considered miscible. The values of ϵ are always higher in the 60/40 blend, suggesting that the PVME relaxation is more efficiently hindered in this blend. These observations are in contrast with several studies of bimodal and miscible blends. For example, in blends of short deuterated PS chains dispersed in a high molecular weight PS matrix, Tassin et al. found a constant coupling parameter at long times, indicating that the relaxation of the low molecular weight chains is correlated with that of the matrix.²⁶ Significant relaxation coupling has also been found by Saito et al. in the poly(vinylidene fluoride)/poly(methyl methacrylate) (PVDF/PMMA) blends⁹ and by different authors in the PS/PPO system.^{8,10,27} On the other hand, the PS/PVME system might be similar to blends of PMMA with poly(ethylene oxide) (PEO),²⁸ where the $\langle P_2 \rangle$ of PMMA goes through a maximum at 5% PEO content, while the orientation of PEO could not be measured by IRLD, probably because of a very fast relaxation rate.

In their theory, Doi and Edwards have suggested that the relaxation of an entangled polymer melt can be described as a sum of exponential functions.²⁹ Messé et al. have also shown that a three-term exponential decay function gives the best fit with a minimum number of adjustable parameters.^{10,15} Using the same procedure, the characteristic relaxation times of both PS and PVME in the blends have been determined from the relaxation curves measured by PM-IRLD at a stretching rate of 100 cm/min. The relaxation times (τ) and the

Table 1. Relaxation Times of PS and PVME in the Miscible PS/PVME Blends after a Rapid Deformation at $T_g + 15$ and 100 cm/min

	PS	90/10 PS	80/20 PS	70/30 PS	60/40 PS	60/40 PVME	70/30 PVME
τ_1 (s)	3	7	7	11	17	14	6
τ_2 (s)	70	90	100	180	230	205	110
τ_3 (s)	19500	12800	9800	6400	8900	6100	2900
A_1	0.020	0.021	0.021	0.027	0.023	0.016	0.016
A_2	0.007	0.011	0.018	0.025	0.030	0.016	0.012
A_3	0.019	0.019	0.019	0.028	0.053	0.015	0.006

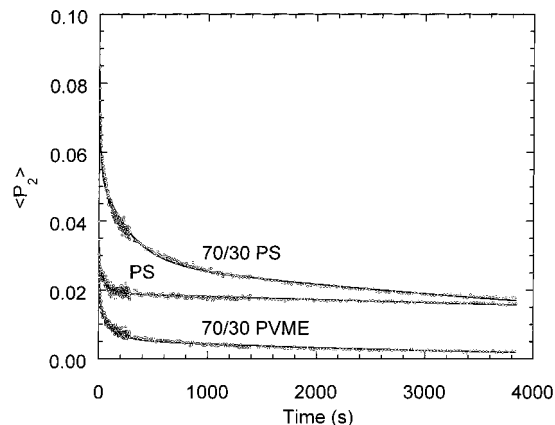


Figure 9. Examples of the fits of relaxation curves using a triple-exponential function, after a deformation at $T_g + 15$ and at 100 cm/min.

preexponential factors (A) for PS in all blends and of PVME in the 70/30 and 60/40 blends are given in Table 1, and examples of fits are given in Figure 9. The experimental error on these times is estimated to ± 2 and ± 20 s for τ_1 and τ_2 , respectively. As expected, a larger relative error is observed for τ_1 in the PS-rich blends because the deformation time (1.3 s) cannot be neglected. For PS, the first relaxation time ranges from 3 to 17 s and shows a regular increase upon the addition of PVME in the blends. Similarly, τ_2 varies gradually from 70 s in pure PS up to 230 s in the 60/40 blend as compared to the 70/30 blend, i.e., 14 and 210 s in the first case as compared to 6 and 110 s for the second one. These results are in agreement with Figures 3 and 6, in which hindered relaxations were observed for both PS and PVME in the PVME-rich blends. The results of Table 1 also show that the relaxation of PVME is significantly faster than that of PS for the same blend, especially in the 70/30 blend. Even though the third experimental relaxation time is generally longer than our experimental time scale because of the high molecular weight of the PS used in this study, Table 1 reveals that there is a semiquantitative regular decrease of τ_3 for PS with the increase of PVME in the blends. This could be related to a dilation of the tube surrounding the PS chains in the blends, due to the faster relaxation rate of PVME.

According to Messé et al., τ_1 and τ_3 values obtained from PM-IRLD experiments for PS of different molecular weights could be related to τ_A and τ_B of the Doi-Edwards model.¹⁵ The first experimental time would then be the longest Rouse relaxation time associated with the local relaxation of segments between entanglement points, and the third experimental relaxation time would consist of the retraction of the chains inside their deformed tube. The origin of the second experimental time is still unclear at this moment. Since the first

relaxation time, in the Doi–Edwards framework, is molecular weight independent, it can be compared with literature values. It has been shown that the first relaxation time of PS at 120 °C should theoretically range between 0.8 and 11 s.^{30,31} Experimentally, Tassin and Monnerie have reported for PS at $T_g + 15$ (about 120 °C) a τ_1 of 5.6 s,³¹ while Messé et al. have obtained directly, at the same temperature, a value of 2 s using dynamic birefringence.¹⁵ These results are in good agreement with the value of 3 s obtained here by PM-IRLD. The only relaxation times available in the literature for PS in PS/PVME blends were obtained by Abtal and Prud'homme at $T_g + 10$ by IRLD from deformation curves.⁷ They determined τ_B values ranging from 300 s for pure PS of molecular weight 300 000 up to 650 s for a 60/40 blend. Assuming the validity of the Doi–Edwards model, these results yield a τ_1 value between 0.5 and 1.3 s, slightly below the values obtained directly in this study.

The results obtained in this work on PS/PVME blends can be interpreted at the molecular level from different points of view. A variation of the friction coefficient has often been invoked to explain the orientation and relaxation behavior of chains in polymer blends. It has been suggested that the strength of the specific interactions between the methoxy group of PVME and the phenyl ring of PS is weak at low PVME content but stronger at compositions over 30% PVME. For instance, Han et al. have measured the interaction parameter χ_{12} over the whole composition range and found a larger negative value in blends above 30% PVME.³² An increase of the friction coefficient between the dissimilar polymer chains should lead to a limited mobility of both components and, thus, to a hindered relaxation, as was observed. The higher initial orientation of PS and PVME in the blends could thus be ascribed in part to a larger intrinsic orientation, but also to a slower relaxation as PVME is added into the blend. This factor could also explain the large difference observed between the 80/20 and 60/40 blends. Since the relaxation of PVME and PS is significantly different, as seen in Figure 7 and Table 1, the interactions could form a temporary or partial network, in which the relaxation of the interacting polymers is hindered, but also in which the “free” PS and PVME do not relax cooperatively. However, we did not observe a maximum in orientation at a composition near the 1:1 ratio of repeat units, around 64% PS. Such change of behavior near the 1:1 ratio was reported in systems with hydrogen-bond interactions such as blends of poly(vinylphenol) with PMMA³³ and PEO.³⁴

A variation of the entanglement density with blend composition can also be considered. From the literature, PVME possesses a smaller molecular weight between entanglements, about 7000–8500 g/mol, than PS at 18 000 g/mol.^{35,36} In the PS-rich blends, most PS chains will interact only with other PS chains, but those in contact with PVME chains should encounter a higher number of entanglements junctions. By increasing the proportion of PVME, the number of chains experiencing this higher entanglement density should also increase, leading to a larger orientation and a hindered PS relaxation. Since the stretching time was short as compared to the determined relaxation times, this variation in entanglement density could explain the results at the end of the deformation process, obtained at time zero. Zhao et al. have defined a critical fraction f_c above which self-entanglement of a polymer can take

place in a blend, as⁸

$$f_c = M_c^0/M_n \quad (3)$$

where M_c^0 is the critical mass for self-entanglement in the bulk polymer and M_n is the molecular weight of the polymer. From eq 3, the minimal fraction for PVME to form self-entanglements is about 28%. This could be related to the appearance of a significant PVME orientation and a large increase of PS orientation above the 80/20 compositions. However, the presence of a maximum orientation in the 50/50 blend cannot be explained by such an entanglement coupling, since the entanglement density should continue to increase in the PVME-rich blends.⁷

Finally, the phase structure of the system could influence the orientation and relaxation dynamics of these polymers. Even if PS/PVME blends are considered miscible, recent studies by either differential scanning calorimetry,³⁷ nuclear magnetic resonance,³⁸ or mechanical or dielectric properties^{36,39} have pointed out the presence of segmental heterogeneities. Such concentration fluctuations could modify the local T_g of regions richer in PS or PVME, thus influencing their deformation and relaxation mechanisms. This effect has also been mentioned in deformation studies of PMMA/PEO²⁸ and PMMA/PVPh³³ blends. The influence of concentration fluctuations in PS/PVME blends will be explored in a forthcoming paper.

Acknowledgment. This work was funded by NSERC of Canada and Fonds FCAR of the Province of Québec. C.P. also expresses his thanks to NSERC for a post-graduate scholarship.

References and Notes

- Ward, I. M. *Structure and Properties of Oriented Polymers*, 2nd ed.; Chapman & Hall: London, 1997.
- Jasse, B.; Koenig, J. L. *J. Polym. Sci., Polym. Phys. Ed.* **1979**, *17*, 799.
- Lefebvre, D.; Jasse, B.; Monnerie, L. *Polymer* **1983**, *24*, 1240.
- Lefebvre, D.; Jasse, B.; Monnerie, L. *Polymer* **1981**, *22*, 1616.
- Lefebvre, D.; Jasse, B.; Monnerie, L. *Polymer* **1984**, *25*, 318.
- Faivre, J. P.; Jasse, B.; Monnerie, L. *Polymer* **1985**, *26*, 879.
- Abtal, E.; Prud'homme, R. E. *Macromolecules* **1994**, *27*, 5780.
- Zhao, Y.; Prud'homme, R. E.; Bazuin, C. G. *Macromolecules* **1991**, *24*, 1261.
- Saito, H.; Takahashi, M.; Inoue, T. *J. Polym. Sci., Part B: Polym. Phys.* **1988**, *26*, 1761.
- Messé, L.; Prud'homme, R. E. *J. Polym. Sci., Part B: Polym. Phys.* **2000**, *38*, 1405.
- Buffeteau, T.; Desbat, B.; Pézolet, M.; Turlet, J. M. *J. Chim. Phys. Phys.-Chim. Biol.* **1993**, *90*, 1467.
- Marcott, C. *Appl. Spectrosc.* **1984**, *38*, 442.
- Buffeteau, T.; Natansohn, A.; Rochon, P.; Pézolet, M. *Macromolecules* **1996**, *29*, 8783.
- Buffeteau, T.; Pézolet, M. *Appl. Spectrosc.* **1996**, *50*, 948.
- Messé, L.; Pézolet, M.; Prud'homme, R. E. *Polymer*, in press.
- Bank, M.; Leffingwell, J.; Thies, C. *Macromolecules* **1971**, *4*, 44.
- Garcia, D. *J. Polym. Sci., Polym. Phys. Ed.* **1984**, *22*, 1773.
- Mirau, P. A.; White, J. L.; Heffner, S. A. *Macromol. Symp.* **1994**, *86*, 181.
- Nishi, T.; Wang, T. T.; Kwei, T. K. *Macromolecules* **1975**, *8*, 7.
- Nishi, T.; Kwei, T. K. *Polymer* **1975**, *16*, 285.
- Chabot, P. Ph.D. Thesis, Université Laval, Québec, Canada, 1991.
- Lafrance, C.-P.; Nabet, A.; Prud'homme, R. E.; Pézolet, M. *Can. J. Chem.* **1995**, *73*, 1497.
- Cole, K. C.; Ben, D. H.; Sanschagrín, B.; Nguyen, K. T.; Ajji, A. *Polymer* **1999**, *40*, 3505.
- Lafrance, C.-P.; Debigare, J.; Prud'homme, R. E. *J. Polym. Sci., Part B: Polym. Phys.* **1993**, *31*, 255.

- (25) Siesler, H. W.; Hayes, C.; Bokobza, L.; Monnerie, L. *Macromol. Rapid Commun.* **1994**, *15*, 467.
- (26) Tassin, J.-F.; Baschwitz, A.; Moise, J.-Y.; Monnerie, L. *Macromolecules* **1990**, *23*, 1879.
- (27) Kawabata, K.; Fukuda, T.; Tsujii, Y.; Miyamoto, T. *Macromolecules* **1993**, *26*, 3980.
- (28) Zhao, Y.; Jasse, B.; Monnerie, L. *Polymer* **1989**, *30*, 1643.
- (29) Doi, M. *J. Polym. Sci., Polym. Phys. Ed.* **1980**, *18*, 1005.
- (30) Boué, F.; Nierlich, M.; Jannink, G.; Ball, R. *J. Phys. (Paris)* **1982**, *43*, 137.
- (31) Tassin, J. F.; Monnerie, L. *Macromolecules* **1988**, *21*, 1846.
- (32) Han, C. C.; Bauer, B. J.; Clark, J. C.; Muroga, Y.; Matsushita, Y.; Okada, M.; Tran-cong, Q.; Chang, T.; Sanchez, I. C. *Polymer* **1988**, *29*, 2002.
- (33) Li, D.; Brisson, J. *Macromolecules* **1997**, *30*, 8425.
- (34) Rinderknecht, S.; Brisson, J. *Macromolecules* **1999**, *32*, 8509.
- (35) Chun, B. C.; Gibala, R. *Polymer* **1994**, *35*, 2256.
- (36) Pathak, J. A.; Colby, R. H.; Floudas, G.; Jerome, R. *Macromolecules* **1999**, *32*, 2553.
- (37) Bershtein, V. A.; Egorova, L. M.; Prud'homme, R. E. *J. Macromol. Sci., Phys.* **1997**, *B36*, 513.
- (38) Asano, A.; Takegoshi, K.; Hikichi, K. *Polymer* **1994**, *35*, 5630.
- (39) Shimizu, H.; Horiuchi, S.; Kitano, T. *Macromolecules* **1999**, *32*, 537.

MA000288C